

INFLUENCE OF THE TEMPERATURE LONGITUDINAL PROFILE IN THE VARIATION OF THE MECHANICAL PROPERTIES OF HEAVY PLATE PROCESSED BY ACCELERATED COOLING*

Davidson Marcos de Oliveira¹

Antonio Adel dos Santos²

Vicente Tadeu Buono³

Abstract

The benefits of using the controlled rolling process followed by accelerated cooling (TMCP), currently used in the main rolling mills in the world are already well known and metallurgically based. The need to obtain mechanical properties with a high degree of homogeneity means that in some situations the ends of the rolled material are discarded, negatively affecting the metallic yield of the process. Therefore, this work focused on the determination of the mechanical properties variation at the ends of thick plates processed by TMCP of steels for application in oil and gas pipelines, in order to map the extent of these differences and to correlate them with the microstructure obtained, the profiles of temperature and cooling rates in these regions. To perform the work, two slabs of the studied material were rolled, and the temperature profile was recorded along the plate in the controlled rolling and accelerated cooling processes. The ends of the material were sampled in sections at every 100 mm and subjected to tensile test, hardness and the Charpy V-notch impact test, as well as dilatometry and microstructure evaluations. For the used process conditions, the results indicated the formation of a banded microstructure, basically consisting of polygonal ferrite and bainite, occasionally containing small fractions of perlite. The mechanical properties in the top and the base were higher than the values found in the plate middle, justified by the microstructure found. The work allowed understanding the relationship between the mechanical properties, microstructures and process conditions at the ends, helping the team to improve the process in order to result in a high degree of homogeneity of the product and, thus, lead to optimization of the metallic yield.

Keywords: Accelerated Cooling, Mechanical Properties, Longitudinal Profile of Temperature.

¹ Production Engineer, Specialist in Statistics, MBA in Process Management and Quality; CQE / ASQ; Full Production Engineer, Technical Management Laminations, Usiminas, Ipatinga, MG.

² Metallurgical Engineer, DSc., CQE / ASQ, Senior Research Specialist, Research Center, Usiminas, Ipatinga, MG.

³ Physicist, M.Sc., Dr., Full Professor, Department of Metallurgical and Materials Engineering, UFMG, Belo Horizonte, MG, Brazil.

1 INTRODUCTION

The use of Accelerated Cooling in the heavy plates began in 1980. Since then, the benefits from its application originated a world effort in the research and development field. One of the challenges of this process is the homogeneity of the physical and metallurgical properties along the material, because its variation generate different characteristics in the temperature longitudinal and transversal profiles of the material, hence also in its mechanical properties^(1,2), that might be leading to excessive discards in the plate.

To ensure that plates produced meet the project specification, it is necessary to discard the ends of the plate, and this negatively affects the metallic yield.

Thus, the length of a slab to be rolled must be carefully planned so that after the rolling process all the discards are made and there is still a useful length that allows the cutting of the heavy plates to the desired dimensions by the customer and optimally, in order not to compromise its metallic yield.

Part of the discarding is due the mechanical properties been different in the ends if compared to specified range, which depends on the microstructure and thus on the local thermal evolution of the plate.

Most of the work on steels produced by accelerated cooling consider, in their analyzes, the average rolling temperature along the plate length^(3,4,5). Therefore, to adjust the discards, it is necessary to study what happens at the ends of the plate, verify the obtained microstructures and the associated mechanical properties. In this sense, this work is focused on the determination of this longitudinal thermal profile and its influence on the mechanical properties along the plate, with emphasis on its extremities.

2 MATERIAL AND METHODS

2.1 Material

Two plates of APIX70MPSL2 grade, used in tube manufacturing, were employed in this study. The chemical composition of the plates was based on the standard API - 5L⁽⁶⁾ and the target values can be found in Table 1.

Table 1. Chemical Composition (wt.%) API-5L⁽⁶⁾

C	Si	Mn	P	V+Nb+Ti
≤0.12	≤0.45	≤1.70	≤0.025	≤0.15

The slabs with dimension of 252 mm x 1954 mm x 3550 mm, (thickness x width x length), were laminated to obtain three plates with final dimension of 12.70 mm x 2850 mm x 12050 mm. The sizing was performed to meet the losses during the process, according to Figure 1.

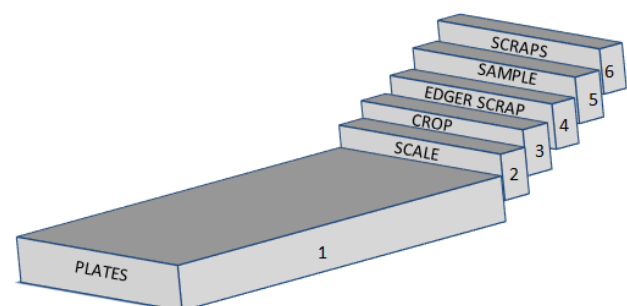


Figure 1. Foreseen discards on the selected plates

2.2 Industrial Processing

The slabs were reheated under controlled conditions of time and temperature, Figure 2, aiming to reach the complete solubilization of the microalloyed elements, according to Schiavo's study⁽⁴⁾, showing the finish reheated temperature (F_{HT}) and solubilization temperature (S_T).

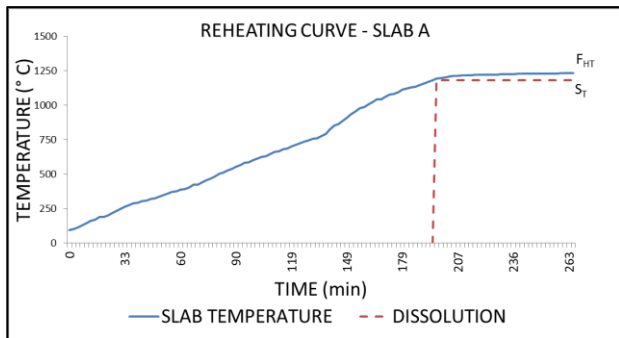


Figure 2. Slab reheating curve

Rolling through the Thermal Mechanical Controlled Process (TMCP) method was performed with eleven roughing passes and heavier reductions, with an average reduction of 18 mm per pass. After the holding pass, the finishing rolling was accomplished with thirteen passes. Figure 3 shows the difference of temperature between per roll passes temperatures obtained at each roll pass.

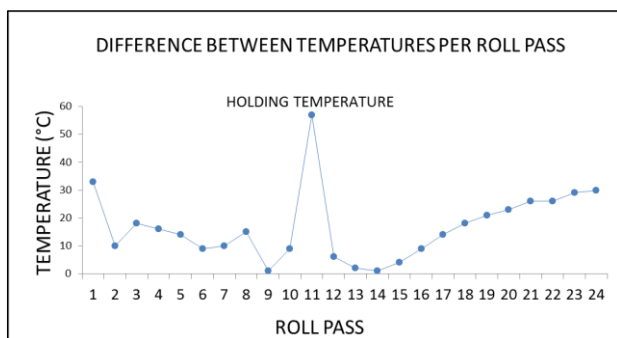


Figure 3. Schematic representations of temperature per roll pass.

The accelerated cooling was initiated at a temperature below AR_{3} , with flows below $0.6 \text{ m}^3/\text{m}^2/\text{min}$ at the beginning of the process and below $2.2 \text{ m}^3/\text{m}^2/\text{min}$ in the final cooling zones, which promoted a cooling rate below $80 \text{ }^\circ\text{C}/\text{s}$. The temperature profiles along the plate were taken at the rolling mill outlet positions (finishing rolling temperature, F_{RT}), at the inlet and outlet of the accelerated cooling process (start cooling and finish cooling temperatures, S_{CT} and F_{CT} respectively). The records were obtained from the sensors installed in these positions and used for process control.

2.3 Mechanical Properties

Samples of the plates were taken in positions as shown in Figure 4.

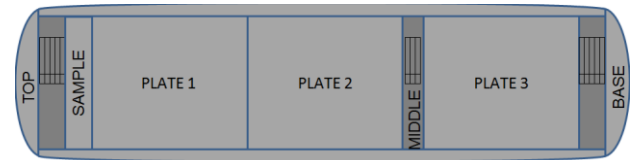


Figure 4. Rolled plate outline and sampling region

At top and base of the plates, a sample of $500 \text{ mm} \times 600 \text{ mm}$ (length \times width) was taken and divided into five specimens of $100 \text{ mm} \times 600 \text{ mm}$, while in the middle of the plate divided in three specimens of $100 \text{ mm} \times 600 \text{ mm}$, was taken as shown in Figure 5.

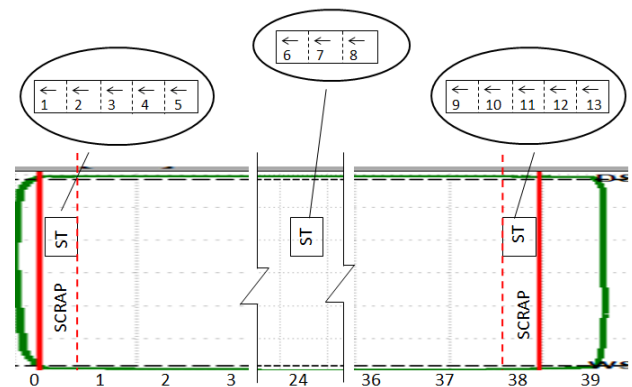


Figure 5. Sample cut section details

Tensile tests at room temperature were performed in the Instron machine of 1200 kN capacity, in specimens transverse to the rolling direction, made according to ASTM A370/17a⁽⁷⁾.

Specimens for the Charpy-V-notch (CVN) impact test, performed at $-20 \text{ }^\circ\text{C}$, also in the transverse direction, were prepared according to ASTM A370/17a⁽⁷⁾.

2.4 Microstructure and Hardness

Longitudinal metallographic sections were prepared at six positions on the end subsamples of the plate and at one position on the plate middle, as shown in Figure 6.

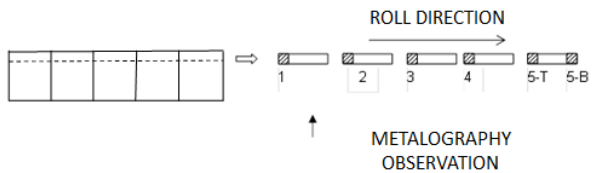


Figure 6. Sampling for the execution of microstructure and hardness tests in the top and the base of the last plate of the as rolled slab.

Since the total length of the end sample was 500 mm, with each sub-sample measuring 100 mm, the measured distance is about 600 mm from the first to sixth section. In the sample withdrawn in the center of the plate only one specimen was removed.

Microstructure analysis was performed after section attack with 4% Nital reagent, followed by observation under Optical Microscope, (OM), and Scanning Electron Microscope, (SEM), with Inlens detector. Determinations of Vickers hardness HV 3 kgf also in the $\frac{1}{4}$ of the thickness were performed in all sections.

2.5 Dilatometry

Cylindrical specimens of 5 mm diameter per 10 mm length were prepared and tested by dilatometry on the Bähr Dil 805D dilator, with the deformation and cooling modes.

The objective was the determination of the continuous cooling transformation diagram (CCT) of the steel and the effect of finishing rolling temperatures, start and finish cooling temperatures in the microstructure and hardness.

Six thermomechanical cycles were selected according to Figure 7. After austenitization at 920 °C the specimens were cooled to the F_{RT} , where double deformation was applied, cooled slowly to the S_{CT} , cooled rapidly to the F_{CT} , and from there, cooled slowly to the room temperature.

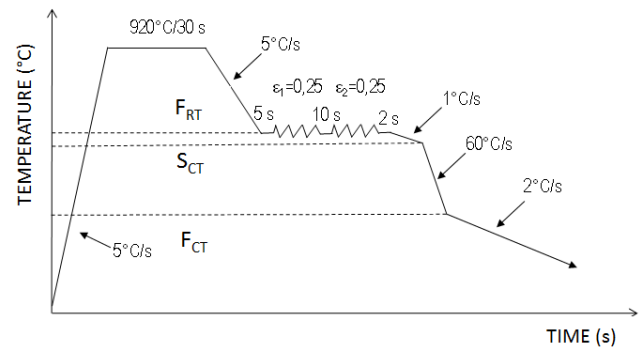


Figure 7. Scheme of the thermomechanical cycle applied in the dilatometric tests.

The conditions of the six tests are shown in Table 2.

Table 2. Conditions of dilatometric tests with application of deformation on the specimen

Test	$F_{RT}(^{\circ}C)$	$S_{CT}(^{\circ}C)$	$F_{CT}(^{\circ}C)$
1	750	710	470
2	750	710	420
3	750	710	370
4	720	690	470
5	720	690	420
6	720	690	370

3 RESULTS AND DISCUSSION

3.1 Temperature Profiles

The behavior of the temperature profile occurred as expected, that is, with a decrease in the top and base of the plates due to the greater thermal loss for the environment in this region, see graph in Figure 8

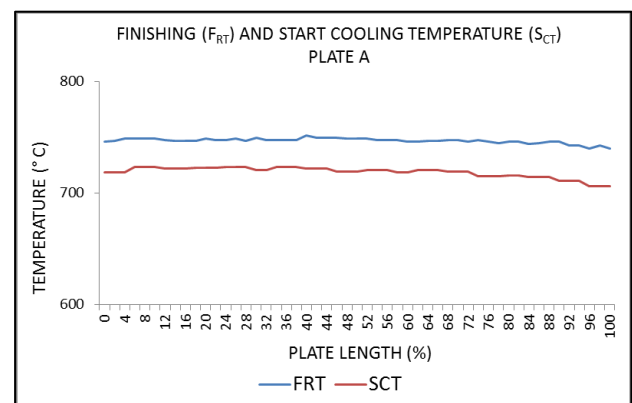


Figure 8. Temperature profiles of finishing rolling and start cooling along the length of the plate.

It can be observed that the S_{CT} tends to maintain the profile obtained in the F_{RT} after the lamination processes.

The F_{CT} used for process control is getting by the median of overall measures at the center of the plate, collected along the length, whose results were plotted in the graph of Figure 9.

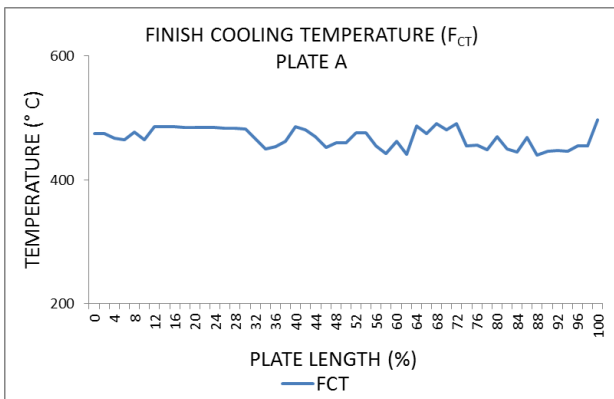


Figure 9. Finish cooling temperature profile along the length of the plate.

The Figure 10 presents the thermography after accelerated cooling of plate A.

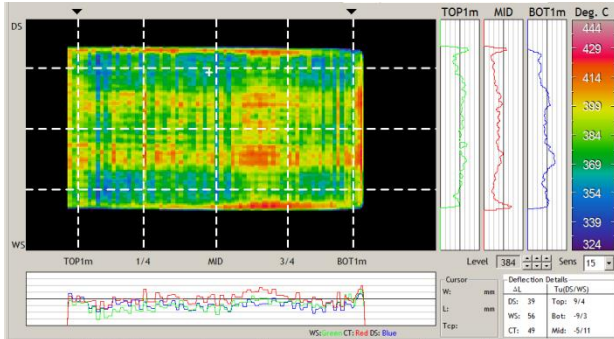


Figure 10. Plate thermography after accelerated cooling.

3.2 Mechanical Properties

Figures 11 and 12 show the results of tensile tests of the plates, referred to as A and B. It is noted that the plate middle, has slightly lower mechanical strength than the top and base. In these, there is no abrupt change in yield strength (YS) and tensile strength (TS). All values obtained were above the minimum specified in standard for steel.

The average YS values were 553 and 590 MPa at top of plates A and B, 511 and

530 MPa in the middle region and 551 and 558 MPa at the base of plates A and B, respectively. This same behavior was observed for the TS, except that with a smaller difference between the middle and the base of the plates.

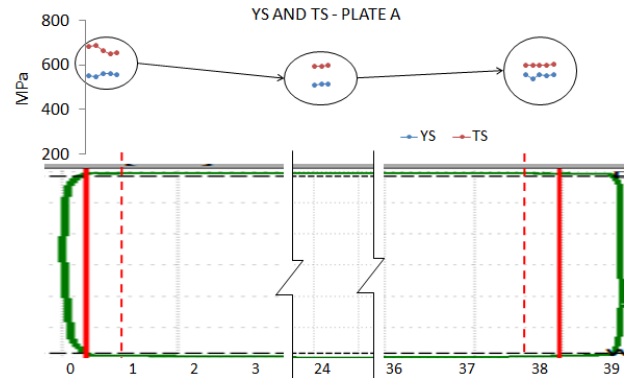


Figure 11. Values of YS and TS along the length of plate A.

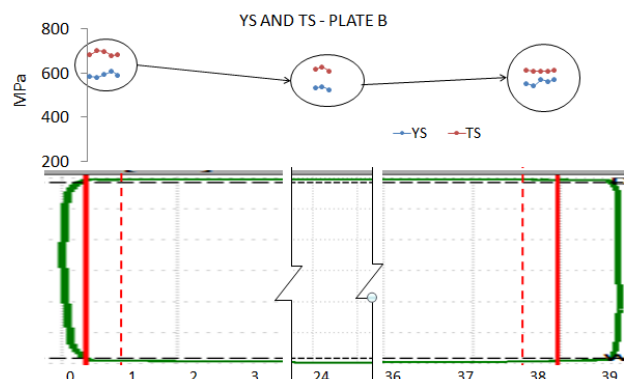


Figure 12. Values of YS and TS along the length of plate B.

The Total Elongation, (TE), remained between 35% and 40% throughout the material and the energy absorbed in the CVN was high and above the specification in all positions, according to Table 3.

Table 3. Mean result of tensile test and CVN tests by region of the plates.

		YS MPa	TS MPa	TE %	CVN J
A	Top	553	667	37	352
	Middle	511	593	38	351
	Base	551	598	40	333
B	Top	590	687	35	297
	Middle	534	621	40	270
	Base	558	609	39	302

3.3 Microstructure and Hardness

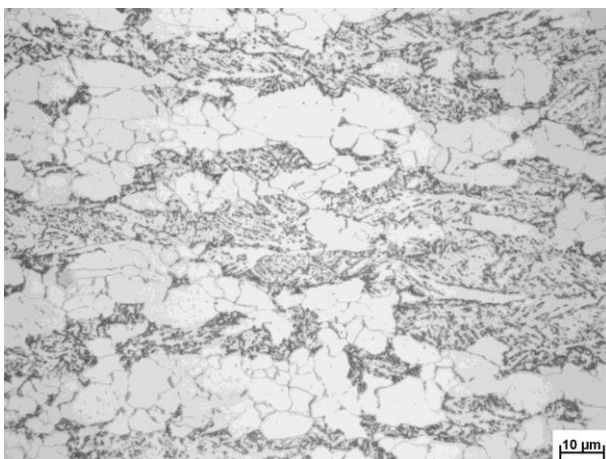
Microstructure images observed in OM and SEM are shown in Figure 13. There was good homogeneity of microstructure in the thickness direction of the plate, so that only the record performed in the center of the thickness is presented.

In the middle of the plate, the microstructure was constituted of polygonal ferrite and bainite as second phase, in an aligned way, Figure 13-(a). Viewed in the SEM, Figure 13-(b), the presence of ferrite and bainite is clearly defined. Indeed, the expected microstructure in steels processed by TMCP is fine ferrite and bainite, since the high cooling rate in this equipment promotes the formation of bainite, in detriment of perlite, while the sufficiently high F_{CT} prevents the formation of martensite.

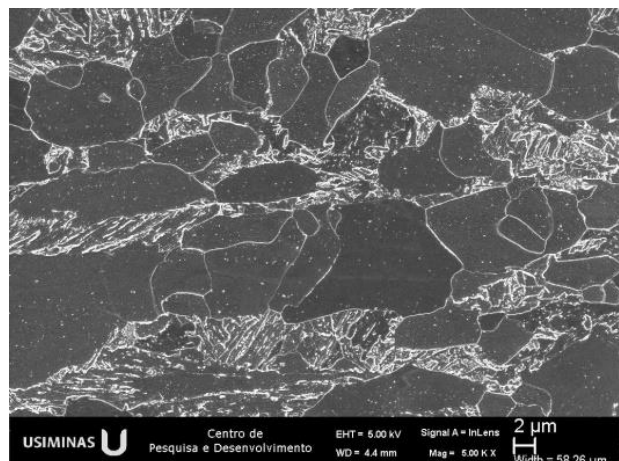
In the sample withdrawn at the top of plate A, the microstructure is composed of ferrite and banded bainite, as can be observed in Figure 13-(c) and 13-(d). Note the more intense banding and greater fraction of bainite in the center of the thickness of the plate, associated with the typical central segregation of the material.

At the base of the plate, Figures 13-(e) and 13-(f), the microstructure consists of ferrite and bainite, but compared to the top of the plate, the bainite is less compact with wider ferrite slats and, in general, there is apparently a higher proportion of ferrite in the microstructure.

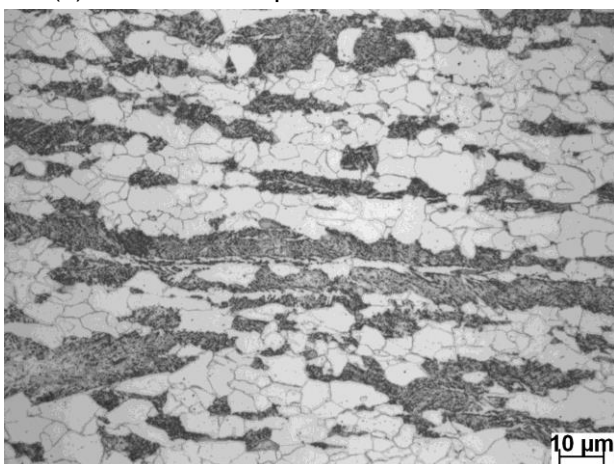
Actually, there is no great microstructural difference between the top, middle and base of the plate, which is in accordance with the mechanical properties obtained.



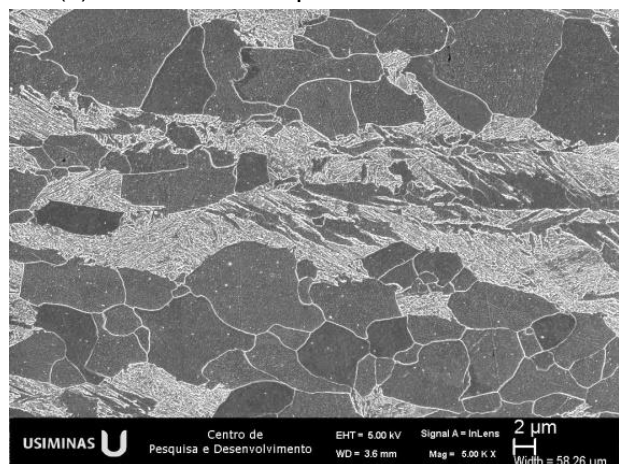
(a) OM – middle plate



(b) SEM – middle plate



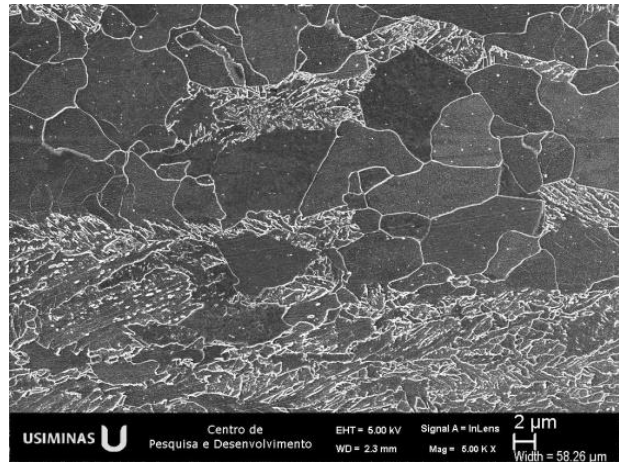
(c) OM – top of the plate



(d) SEM – top of the plate



(e) OM – base of the plate

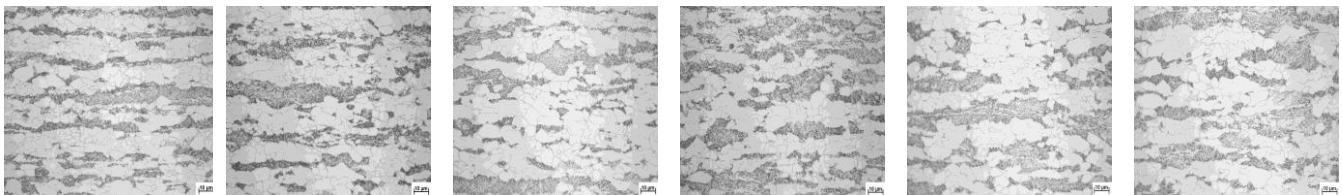
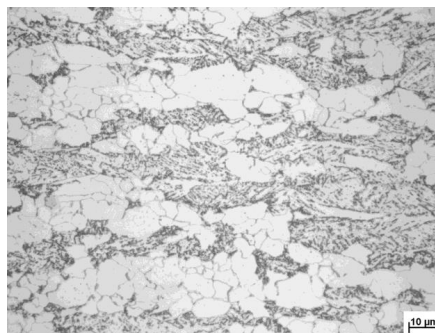
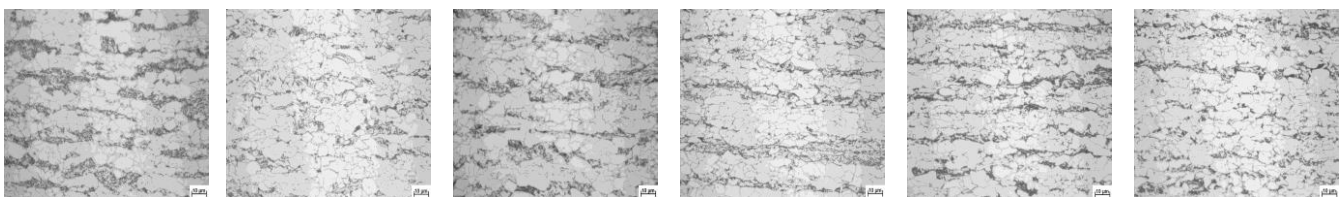


(f) SEM – base of the plate

Figure 13. Microstructure on top, middle and base of plate A

The sequence of images of Figure 14 shows the evolution of the microstructure, viewed from the OM, at the top of plate A, in the region of 600 mm from the cut going towards its end. In Figure 15 the microstructure is shown in the middle of the plate and in Figure 16, the evolution of

the microstructure at the base, from the cutting section, going towards the end corresponding to the base of the plate. There is no significant variation of microstructure in this region, consistent with the small variation of tensile properties shown in Figures 11 and 12.

**Figure 14.** Microstructure of the top of the plate A of 1000X to 1/4 of the thickness.**Figure 15.** Microstructure of the middle of the plate A of 1000X to 1/4 of the thickness**Figure 16.** Microstructure of the base of the plate A of 1000X to 1/4 of the thickness

Hardness values measured at $\frac{1}{4}$ of the thickness in the samples (mean of 10 determinations) are shown graphically in Figures 17 and 18, in plates A and B, respectively.

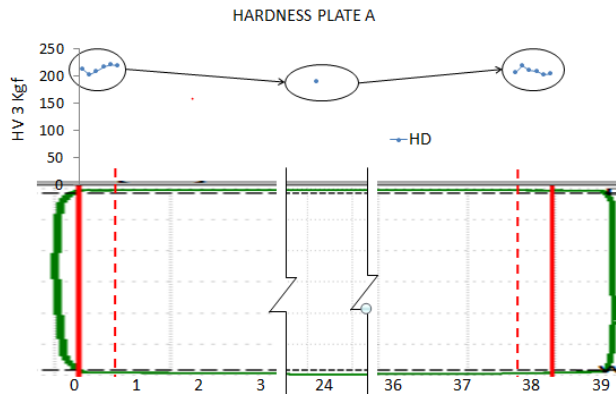


Figure 17. Medians hardness values in plate A

The hardness in the middle of the plates was practically the same, close to 190 HV. In the regions of the analyzed on the top and base, the hardness oscillated in the range of 5 to 26 HV, without a definitive tendency of variation with the position, always remaining above the value of the middle of the plate.

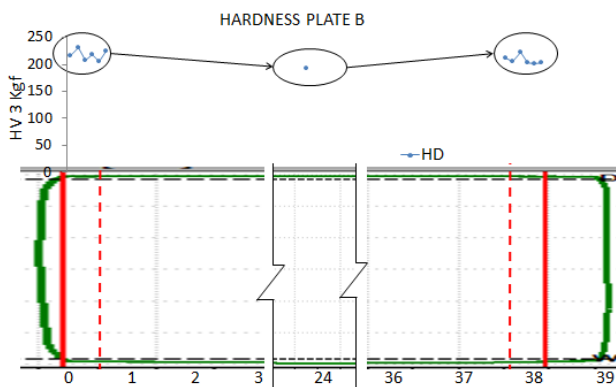


Figure 18. Medians hardness values in plate B

In general, in the region of the base of the plate the hardness was slightly lower, except in an analyzed section. This finding is consistent with the observation of the microstructure, which presented a tendency of higher ferrite fraction, formation of superior bainite and some occurrences of crumbled perlite in the sections of the base of the plate. These microstructural characteristics are associated with higher phase

transformation temperatures, meaning that, either the cooling start temperature was higher, or the lower cooling rate, or both in this sense.

3.4 CCT Diagram and Dilatometric Tests with Deformation

The CCT diagram constructed of the steel under study is shown in Figure 19. The microstructure consisted predominantly of ferrite, with smaller amounts of bainite, martensite and perlite. The perlite fraction decreases with increasing cooling rate until the rate is reduced to around 25 °C/s. On the other hand, the fractions of bainite and martensite increase with the cooling rate, with martensite increasing more significantly at rates above 20 °C/s. Note that the banded microstructure has disappeared to a rate above 10 °C/s. Although the CCT diagram is an useful tool to understand the effect of the cooling rate on the microstructure and hardness of the steel, its construction from the recrystallized austenite, as in this case, does not reproduce the properties of the industrially processed plates. Two major differences occur in this case. First, austenite is encrusted in the industrial process before the cooling start; Second, accelerated cooling is interrupted in the bainitic field, contrary to the direct cooling to the environment temperature in the CCT diagram.

Thus, the tests were performed by dilatometry with deformation, subjecting the recrystallized austenite after the soaking at 900 °C to the deformation already in the intercritical region, Figure 9. The aim was to try to identify deformation and cooling conditions that reproduced the microstructure and hardness obtained in the samples of middle and the top and base of the plate.

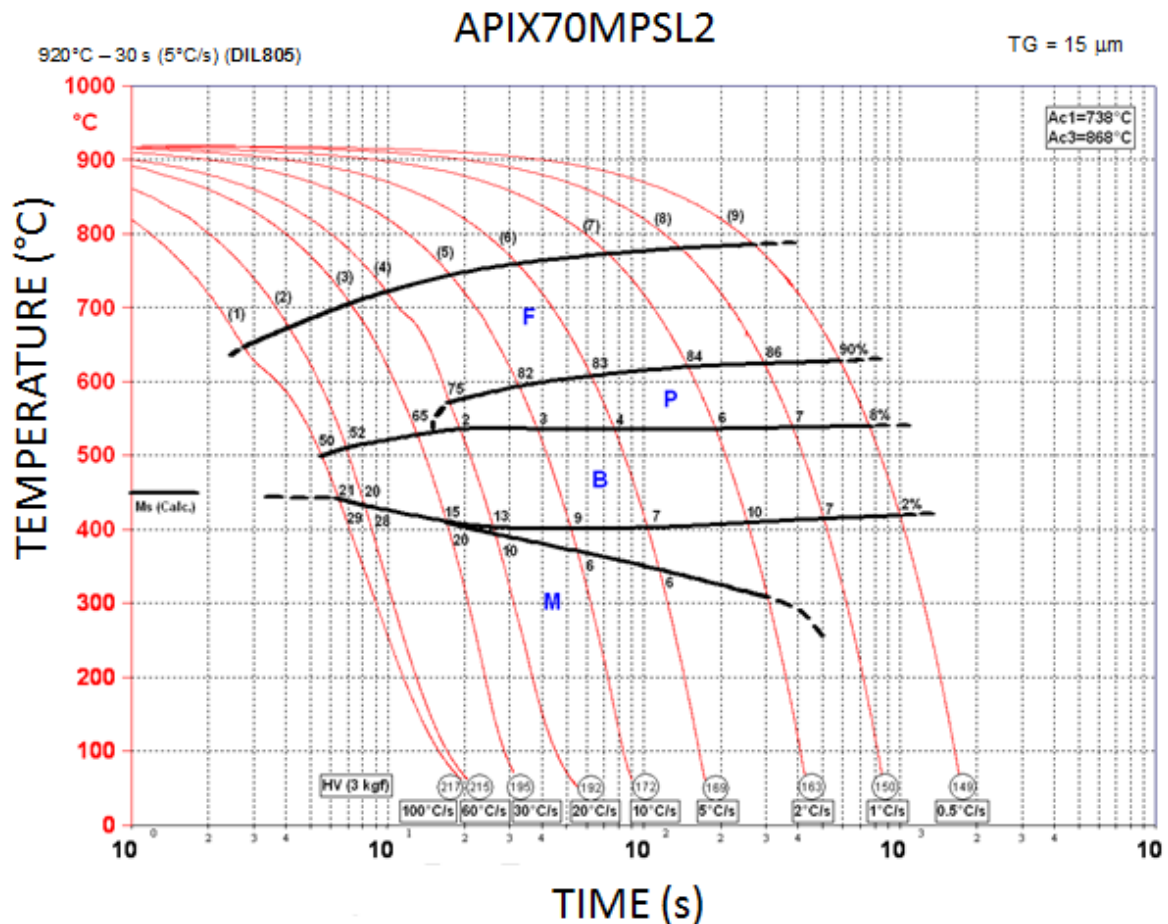


Figure 19. CCT diagram of APIX70MPSL2 steel under study

In Figure 20 is shown, as an example, the microstructure obtained in the specimens tested with $F_{RT} = 720$ °C, $S_{CT} = 690$ °C and $F_{CT} = 420$ °C.

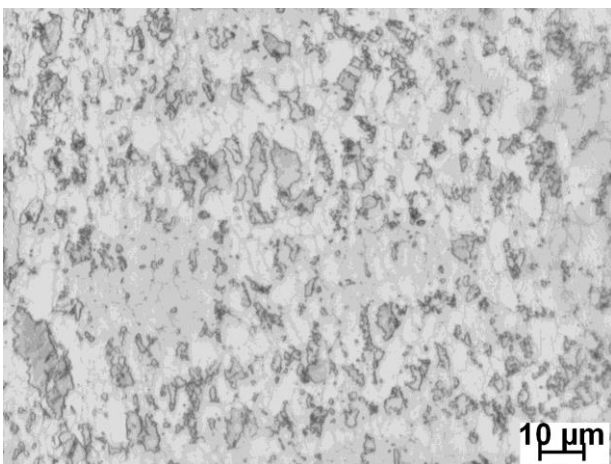


Figure 20. Microstructure obtained at the specimen tested at $F_{RT} = 720$ °C, $S_{CT} = 690$ °C and $F_{CT} = 470$ °C

The microstructure was very refined and constituted of ferrite and second

constituent, which it was not possible to identify with the OM analysis only. This constituent is, probably, a mixture of bainite and martensite. It is interesting to note that the obtained microstructure is similar to the one of the specimens tested for the construction of the CCT diagram, in other words, not yet representing the microstructure of the industrial plate.

This indicates that deformation tests with dilatometry should be done in such a way as to simulate the complete thermomechanical cycle of the rolling, including reheating at high temperatures for dissolution of precipitates, roughing and finishing rolling, followed by accelerated cooling.

The hardness values of the specimens tested in the six different conditions are given in Table 4, in terms of mean and standard deviation, and graphically in Figure 21.

Table 4. Hardness of specimens tested by dilatometry with deformation, simulating the steps of finishing and accelerated cooling (HV 3 kgf).
Condition: F_{RT}, S_{CT} and F_{CT}.

Condition	Mean	SD
750-710-470	208.8	8.7
750-710-420	204.8	7.1
750-710-370	217.0	6.4
720-690-470	215.2	4.3
720-690-420	218.4	8.4
720-690-370	225.4	6.1

There is no great variation of hardness with the test conditions, but there is clearly a slight tendency for it to increase with the reduction of the finishing rolling and accelerated cooling temperature.

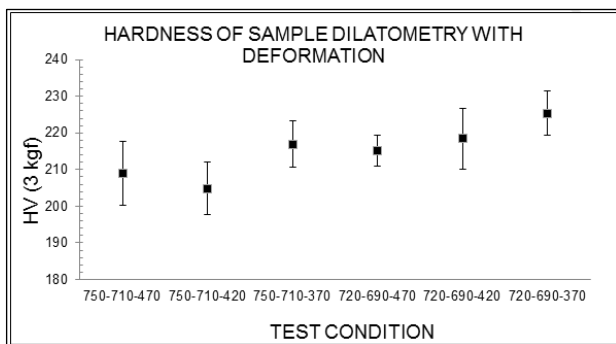


Figure 21 Hardness of the specimens tested by dilatometry with deformation, simulating the steps of finishing and accelerated cooling.

In general, this trend was reported before in the literature⁽⁸⁾. It is interesting to note that the hardness values are slightly higher than those obtained in the CCT diagram. For example, in this diagram, by cooling the specimen between 60 °C/s and 100 °C/s, the hardness reached a maximum of 217 HV, while in the deformation test, the accelerated cooling was achieved at 60 °C/s, the hardness reached 225 HV. In addition, the values obtained for the simulated conditions with low finishing temperature and/or cooling resulted in hardness in the range of 200 HV to 225 HV, exactly the hardness range obtained in the end samples of the plate, Figures 3.15 and 3.16.

On the other hand, in the middle of the plate, with target values of F_{RT} and S_{CT} of 750 °C and 720 °C respectively, the

hardness was around 190 HV, which is below that obtained in the deformation dilatometry simulation, which was next to 210 HV. However, dilatometry simulation results confirm that lower finishing mill temperatures and / or accelerated cooling tend to increase the hardness and hence the strength of the material. This indicates, as expected, that the end regions of the plate are processed at lower temperatures, possibly 30 ~ 50 °C below of middle, resulting in increased hardness.

4 CONCLUSION

The longitudinal temperature profile in the studied plates showed a slight decrease in the ends, in relation to the middle, without sudden oscillations. With that, a small effect on the microstructure and on the mechanical properties was observed. Additionally, the profile in later steps maintain the characteristics of the previous steps.

The microstructure found in the discard regions was banded and consisted basically of polygonal ferrite and bainite, with some similarity to that obtained in the middle plate.

Both the hardness and the mechanical properties at the ends of the plates oscillated, without exhibiting a specific rise or fall behavior along the edge but remained somewhat above the values of the middle and above the specified value in the standard, on the studied steels.

These results indicate that, from the point of view of mechanical properties, the discard region can be optimized, since the obtained variations do not behave abruptly along the ends region.

The dilatometry tests, with or without deformation, with partial thermomechanical cycles, that is, with austenitization around 900 °C, did not adequately reproduce the microstructure of the rolled slabs, indicating that it is necessary to perform the complete cycle from the reheating of the plate.

REFERENCES

- 1 SCHWINN, V., BAUER, J., FLUSS, P., KIRSCH, H.J., AMORIS, E. Recent Developments and applications of TMCP steel plates. *Revue de Métallurgie*. Paris, 108, 283–294, 2011.
- 2 ARAÚJO, C.S. Revisão Bibliográfica sobre Resfriamento Acelerado de Chapas Grossas. Relatório Parcial de Estudo de P&D. 2006.
- 3 FLORES, W. D. et al. Variação de Propriedades Mecânicas em Tubos a partir de Chapas Produzidas via CLC. Relatório de Estudo de P&D, 2014. 67 pp.
- 4 SCHIAVO, C.P. Estudo de solubilização do Nb em aços microligados durante o aquecimento de placas. Belo Horizonte: Escola de Engenharia da UFMG, 2010. 130 pp. (Mestrado).
- 5 MURARI, F, D et al. Efeito das Condições de Reaquecimento na Dissolução de Precipitados e nas Propriedades Mecânicas de Chapas Grossas de Aços Microligados. Relatório Final de Estudo de P&D, 2016. 324 pp.
- 6 API SPECIFICATIONS 5L, 46^o Edition, april 2018, P.30
- 7 AMERICAN SOCIETY FOR TESTING AND MATERIALS, Philadelphia. ASTM A370/17a; Standard Test Methods and Definitions for Mechanical Testing of Steel Products. West Conshohocken, 2016.
- 8 TAKEUCHI I., KUSHIDA T., OKAGUCHI S., YAMAMOTO A., MIURA M. Development of high strength line pipe for sour service and full ring evaluation in sour environment. In: 23rd International Conference on Offshore Mechanics and Arctic Engineering, OMAE, Vancouver, BC, Canada, 2004